Geodesy and Geodynamics 10 (2019) 471–476

Contents lists available at ScienceDirect

Geodesy and Geodynamics

journal homepage: http://www.keaipublishing.com/geog

The subduction of the Copiapó aseismic ridge, is the causing of the formation of metallic minerals deposits in north of Chile and Argentina?

Mario Gimenez [a, *], Gemma Acosta [a], Orlando Alvarez [a], Agustina Pesce [a], Federico Lince Kinger [a], Andres Folguera [b]

[a] Instituto Geofísico Sismológico Volponi, FCEFN, Universidad Nacional de San Juan, CONICET, Ruta 12 Marquesado (Jardín de Los Poetas), Rivadavia, San Juan, Argentina
[b] IDEAN-CONICET, Universidad de Buenos Aires, Argentina

ARTICLE INFO

Article history:
Received 4 March 2019
Accepted 12 April 2019
Available online 12 June 2019

Keywords:
Aseismic ridge
Satellite gravity
Ojos del Salado-San Buena Ventura lineament
Metallic mineral deposits

ABSTRACT

The results obtained in this work evince that the metallic mineral deposits located in the northern region of the Chilean-Pampean flat slab (in northern Chile and north-western Argentina), at approximately 27° 30′S, would be related to the subduction of the Copiapó aseismic ridge. The analysis of the gravity anomalies and vertical gravity gradient allows inferring a deflection and truncation of the main trend of the Andean structures at the extrapolated zone of the Copiapó ridge beneath South America. Thus, the general NNE-trend of the Andean structures are rotated locally to an ENE-strike within the area of the Ojos del Salado – San Buena Ventura lineament. We explain that this anomalous behavior of the gravity derived anomalies is related to the deformational effects imprinted by the ridge subduction. Regions with a low subduction angle (<30° to horizontal) are related to large mineralization due to fluids released by dehydration of the subducting crust. In addition, a higher degree of mantle melting could be produced by a thicker oceanic crust. Therefore, we interpret that the processes associated to the subduction of the Copiapó aseismic ridge (emplaced on a thickened oceanic crust due to a local compensation of the seamounts) are the cause of formation and emplacement of big metallic mineral deposits in this region of Chile and Argentina.

1. Introduction

Seamounts, aseismic ridges, hotspot volcanic chains and oceanic plateaus trajectory reconstructions at the western Pacific, have been used to explain the development of the Pampean-Chilean flat subduction zone [1–3].

The ENE-trending Ojos del Salado–Buena Ventura volcanic lineament [7] extends at approximately 27°S for almost 300 km [8,9]. This geologic lineament ranges from the Chilean Central Valley to the eastern Andean front producing a major transverse morphological discontinuity through the chain composed of the highest volcanoes of the world (e.g. the Ojos del Salado dome complex and Tres Cruces and Incahuasi stratovolcanoes, for more details see Bonatti et al. [10]; Mpodozis and Kay [11]; Mpodozis et al. [5]). This lineament is associated with a strong deflection in the Andean drainage divide area from N in the south to ENE in the north imposed by aligned stratovolcanoes and dome complexes that are forming part of the arc front at these latitudes [4] (see Fig. 1). These centers are affected and controlled by normal and right lateral structures with regional extent identified in the field defining a general ENE structural alignment [4–6,12].

* Corresponding author.
E-mail address: mgimenez@unsj-cuim.edu.ar (M. Gimenez).

Peer review under responsibility of Institute of Seismology, China Earthquake Administration.

Production and Hosting by Elsevier on behalf of KeAi

https://doi.org/10.1016/j.geog.2019.04.007

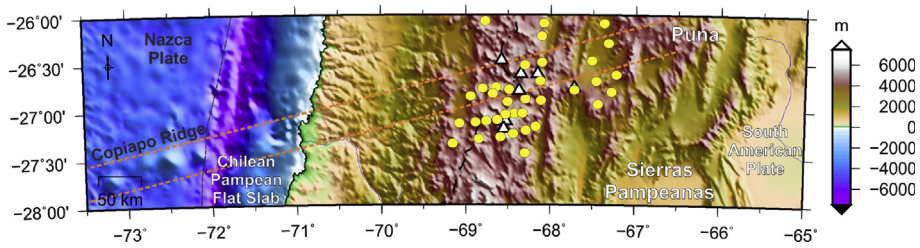

Fig. 1. Shaded digital elevation model at the northern region of de Chilean-Pampean flat slab. White triangles show the southern limit of the active volcanic arc known as Central Volcanic Zone (CVZ). This region around 27.5° S, is the transition zone between the 30°E dipping Nazca plate (to the north) and the flat slab (to the south) where a gap in arc activity is established up to approximately 30°S (Chilean-Pampean flat slab). Yellow circles depict individual centers of the Ojos del Salado-San Buenaventura volcanic lineament that develop from the arc zone to the retroarc area [4–6]. Note the general match between the trend of the extrapolation of the Copiapó ridge beneath the South American plate and the Ojos del Salado-San Buenaventura volcanic lineament.

The relation between the Copiapó ridge subduction and upper plate deformation had been previously suggested by different authors [10,13–15]. In a recent work, Alvarez et al. [3,16] used Earth gravity field data to track the presence of this feature beneath the South American plate. The last authors calculated the gravity anomaly and vertical gravity gradient for the South Central Andes and adjacent offshore region taking the advantage of the relative high spatial resolution of the global gravity field model EGM2008 and the homogeneous precision of GOCE satellite data. Moreover, Mulcahy et al. [17] through earthquake hypocenters recorded in the Andean Southern Puna seismic array (25–28°S, 70–65°W) obtained a refined shape of the Wadati-Benioff zone under the Southern Puna and the northern margin of the Chilean-Pampean flat slab. Their results support high temperature at the base of the lower crust and a hot asthenospheric mantle wedge under the Southern Puna. They found slight differences of the redefined geometry from previous representations in the Southern Puna; being a more pronounced westward bulge of the 100–130 km contours in the region centered near 27°S where the Copiapó aseismic ridge intersects the Chile trench.

Rosenbaum et al. [18], reported a spatio-temporal link between the subduction of the Juan Fernandez ridge in Central Chile and the intense metallogenic activity in this region since the middle Miocene and also to the lateral changes in the spatio-temporal distribution of the metallogenic domains in the area. Alvarez et al. [3] proposed that the subduction of the Copiapó aseismic ridge could have controlled the northern edge of the Chilean-Pampean flat slab, due to higher buoyancy, similarly to the control that the Juan Fernandez ridge exerts in the geometry of the flat slab further south.

In this study, we infer a link between the subduction of the Copiapó ridge in the North of Chile and NW of Argentina, with the intense metallogenic activity in this region since the middle Miocene to the present.

2. Gravity data

We focused this work on the evaluation of the interplay between the subduction of an aseismic ridge (Copiapó) and the mineralization that could produce in the overriding plate. For this, we calculated the gravity anomaly and the vertical gravity gradient in the South Central Andes region from the Earth gravity field model EIGEN-6C4 [19].Earth gravity field models are presented as sets of coefficients of a spherical harmonic approximation of the gravity field up to a maximum degree N_{max} which governs the spatial resolution of the model λ [20–22]. EIGEN-6C4 is developed up to degree/order 2159 with some additional terms up to degree/order 2190, the spatial resolution for the potential field model EIGEN-6C4 becomes equal to $\lambda/2 \approx 9$ km (according to Barthelmes [22]).

3. Gravity anomaly and vertical gravity gradient

In order to analyze the gravity and the gradient field with certain geological features we calculated the vertical gravity gradient and the gravity anomaly [23] in the Southern Central Andes region (Fig. 2). The need for higher resolution justifies the calculation with the EIGEN-6C4 model as satellite only models (e.g. GOCE derived) presents a lower resolution of approximately $\lambda/2 \approx 60$ km (being the degree/order of the spherical harmonic expansion $N = 300$). For calculation we used the data of the model EIGEN-6C4 up to degree/order $N = 2159$ [24] on a regular grid with a cell size of 0.05°. The values were calculated in a geocentric spherical coordinate system at the calculation height of 7000 m to ensure that all values were above the topography.

Both quantities were corrected by the topographic effect in order to eliminate the correlation with the topography. Topographic mass elements obtained from ETOPO1 [25] were approximated with spherical prisms [26–30] of constant density in a spherical coordinates system. The use of spherical prisms is necessary to take into account the Earth's curvature [31–34]. A standard density of 2.67 g/cm^3 was used for continental crust and a density of 1.03 g/cm^3 for the sea water. All calculations were performed with respect to the World Geodetic System 1984 (WGS84). The topographic correction becomes greater (up to tens of mGal/m (Eötvös) for Tzz and up to a few hundreds of mGal for gravity) over the maximum topographic elevations (e.g. the Puna and the Main Andes) and lower over the topographic depressions such as the Chilean trench.

4. Euler Poles

The backtracking technique [35,38–41] allows to rotate seamounts (of known age) back to their presumed origin (e.g. a hotspot), and forward to a final position. We calculated the extrapolated track of the Copiapó ridge (forward) using Euler Poles (Fig. 3) indicating its future development in 2 Ma, and in 8 Ma. The backward calculation indicates a probable origin at

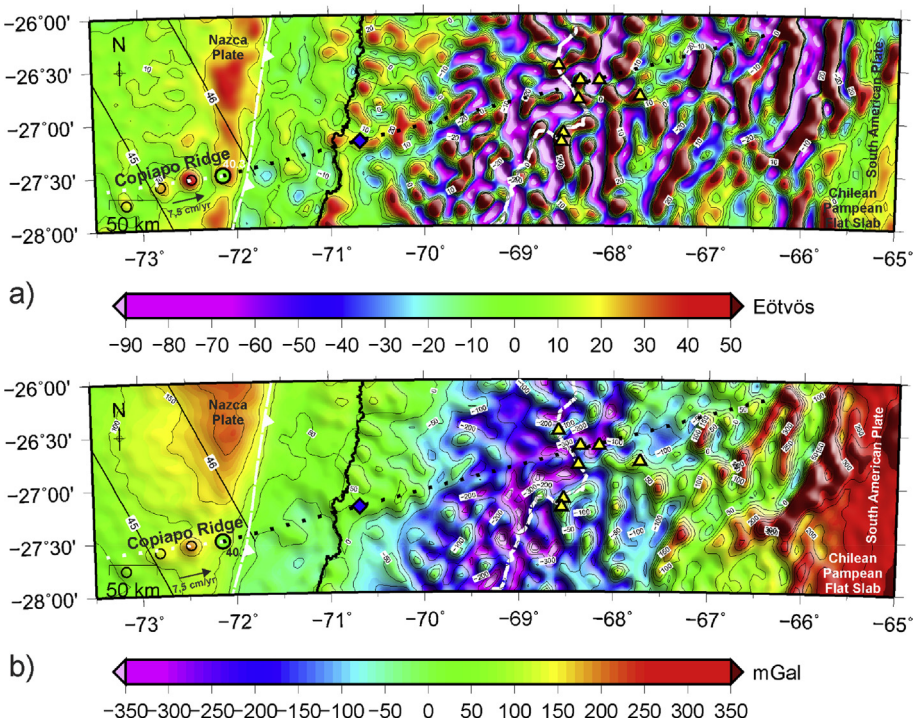

Fig. 2. a) Vertical gravity gradient from EIGEN-6C4 corrected by topographic effect in the region of the Copiapó ridge and Ojos del Salado–Buena Ventura volcanic lineament. b) Gravity anomaly computed from the EIGEN-6C4 model corrected by topographic effect. Superimposed, the track of the Copiapó ridge is indicated backwards in time (white dashed line) and forwards in time (black dashed line). Circles are seamount locations and respective age of the underlying sea floor in million years, from the catalog of Wessel [35]. Solid line indicates oceanic crust ages [36]. Triangles indicate the current position of the active volcanic arc [37].

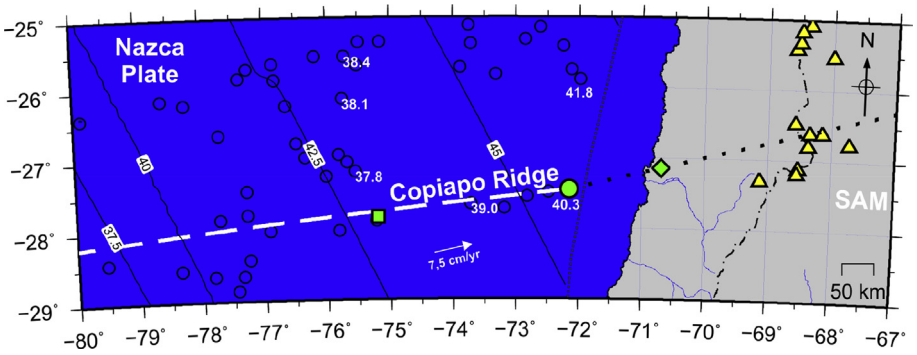

Fig. 3. Reverse and forward reconstruction of the Copiapó ridge trajectories using Müller et al. [36] and DeMets et al. [42] Euler Poles respectively. The square indicate the corresponding position 2 Ma ago for the seamount (circle) located near the trench (Seamount age 40.3 Ma), while the rhomb indicates its future position beneath the continent in 2 Ma. Triangles indicate the current position of the active volcanic arc [37]. Note that the extrapolation of the Copiapó ridge coincides with an eastward migration of the active volcanic arc instead of the gap in magmatic activity, characteristic of the Pampean-Chilean flat slab, observed to the south. Blue circles are seamount locations with the age of the underlying sea floor (Ma) from the catalog of Wessel [35]. Solid lines indicate oceanic crust ages [36].

the Easter (Sala *y* Gomez) hotspot approximately 40 Ma ago. At the latitudes between 26.5°S and 27.5°S is observed a rotation in the general strike of the NNE pattern of the Ga and Tzz anomalies to a general ENE direction. This is interpreted as the expression of a regional rotation in the Andean structures (Fig. 2), circumscribed to a stripe coincident with the extrapolation of the Copiapó ridge beneath the South American Plate (obtained from Euler poles between Nazca and South American plates.

5. Results

In the map of the topography corrected gravity anomaly, the influence of the Andean root is expressed by low gravity values (less than −300 mGal). The positive effect of the oceanic Nazca plate is also observed, reaching its maximum values (more than +200 mGal) at the outer rise area. The Copiapó ridge can be tracked by its well-defined gravity signal, lower than the surrounding oceanic ocean floor.

Seaward of the trench, the outer rise area produced by the flexure of the downgoing Nazca plate, coincides with a positive Ga of about 200 mGal, and with a positive Tzz higher than 25 Eötvös (Fig. 2). The Copiapó ridge is marked by a well-defined Tzz signal higher than 30 Eötvös and a Ga higher than 250 mGal.

Between 26.5°S and 27.5°S, a notorious change in the strike of the general NNE pattern of the anomalies to an ENE-direction is of particular interest, being exhibited by both the Ga and Tzz obtained from EIGEN-6C4 (Fig. 2). This is interpreted as reflecting a change in the Andean structural trend. This change coincides with the extrapolation of the Copiapó ridge beneath the South American plate, when calculating the forward position of the ridge using the present rotation poles between Nazca and South American plates.

The ENE deflected Ga and Tzz obtained from EIGEN-6C4 would be mainly related to the shallowest expression of the deformation as the high frequency gravimetric signal is mainly related to shallower density contrasts (long wavelengths are related to deeper sources).

6. Ridge subduction and mineralization

A seamount or an aseismic ridge acquires different states of buoyancy as enter the trenches. A seamount located on a strong oceanic plate would be regionally supported and, hence, much of its compensation have been removed prior to subduction. Due to a lower buoyancy, such a seamount or aseismic ridge would be less likely to uplift the outermost forearc and, and thus being more weakly coupled to the overriding plate. On the other hand, a seamount formed on a weak plate is more locally compensated, being more bouyant and is more likely to jam producing indentation, a higher degree of faulting and deformation of the continental margin [43].

Studies of seamounts (or aseismic ridges) made by Nishizawa et al. [44] and by Contreras-Reyes et al. [45] using deep seismic reflection along the continental margin, showed that these seamounts are underlain by a thickened oceanic crust. Moreover, P-wave velocity contours are elevated; suggesting that these seamounts have relatively dense cores and that the underlying flexed crust may have been intruded by magmatic material. Baker et al. [14] proposed that the Ojos del Salado lineament may represent a continental extension of the chain of islands and seamounts referred to as the 'Easter Hot Line'.

The Ojos del Salado-San Buena Ventura volcanic lineament represents an anomaly in the pattern of arc-retroarc volcanism at the northern extreme of the Chilean-Pampean flat zone. These volcanic centers are controlled by ENE-oriented regional structures with dip and strike-slip strain components that project into the retroarc zone transversally to the arc front. Moreover, the development of this volcanic lineament coincides with a strong deflection in the fabric of the Andean deformation determined from gravity analyses [3]. Then, neotectonic deformation, volcanic alignments and the deformation patterns at about 27.5°S could be spatially linked to the collision of the Copiapó aseismic ridge. Additionally, convergence direction of this oceanic feature parallels the plate convergence direction between the Nazca and South American plates (78.1° azimuth NE in our study area [46]). This implies that the point of insertion of the Copiapó ridge colliding against the trench does not shift towards the south as reported for the Juan Fernandez ridge further south [1]. Therefore, the deformational imprint over the upper plate is expected to affect a more discrete zone than in the southern ridge collision, producing an ENE-localized deformational zone. This could explain the regional deflection of the gravity anomalies and gradients observed along a discrete stripe. The Andean fabric associated to the flat subduction processes in the region looks unaltered to the north and south of it. Additionally it explains why neotectonic deformation acquires, to the east of the arc front, a predominant E–NE orientation along the Ojos del Salado-San Buena Ventura volcanic alignment.

Kay and Mpodozis [47], expressed that major Miocene Central Andean ore districts (between 22° and 34°S) share common tectonic and magmatic features that point to a model for their formation over a shallowing subduction zone or during the initial steepening of a formerly flat subduction zone. In the region of Copiapó the subduction angle is of about 5°E and the crustal thickness is 60 km [48].

A key ingredient for magmatism and ore formation is release of fluids linked to hydration of the mantle and lower crust above a progressively shallower and cooler subducting oceanic slab. Other ingredient is stress from Nazca-South American plates convergence that results in crustal thickening (in depth) and shortening (W–E) in association with magma accumulation in the crust. Fluids for mineralization are released as the crust thickens, and hydrous, lower crustal amphibole-bearing mineral assemblages that were stable during earlier stages of crustal thickening break down to dryer, more garnet-bearing ones [47].

Following the track of the Copiapó ridge over the continent, are located the most significant mining deposits in Argentina, such as: Farallón Negro (the biggest gold district in this country). Production is under way at Bajo de la Alumbrera, 767 Mt of reserves with 0.51% Cu and 0.64 g/t Au [49] and Farallón Negro 1.5 Mt with grades of approximately 6 g/t Au and 99 g/t Ag [50]. Other locations are under evaluation: Agua Rica with 1457 Mt of measured and indicated reserves with 0.2% Cu cutoff grading 0.44% Cu, 0.03% Mo, 0.19 g/t Au, and 3 g/t Ag (electronic communication, Northern Orion website). In Fig. 4, we show the track of the Copiapó aseismic ridge and all mining districts located in the area.

The mineralization is linked to changes in crustal and lithospheric thickness induced by the evolving geometry of the subducting Nazca plate. Fluids for mineralization that are ultimately derived from the hydrated mantle above the subducting slab are released as wet amphibole-bearing lower crust thickens and transforms into dryer, garnet-bearing crust above a shallowing or recently shallow subduction zone [51]. The mineralization associated to Copiapó ridge took place in the Chilean flat-slab region, as the subduction zone was shallowing [48].

7. Conclusion

The Ojos del Salado-San Buenaventura volcanic lineament presents an anomaly in the pattern of arc and back-arc volcanism at the northern end of the Pampeana flat subduction zone, coinciding with the extrapolation of the Copiapó aseismic ridge. This causes a strong deflection of the Andean deformation factory determined from the gravimetric analysis, which is clearly observed at 27.5°S latitude. This trace produced by the Copiapó ridge under the South American plate is inferred by a gravimetric analysis.

The subduction of the Nazca plate between approximately 27°S to 32°S, in a flat slab configuration with two ridges subducting at its edges (the Copiapó aseismic ridge to the north and the Juan Fernandez ridge to the south), produced one the larger mineralized regions in South America. This "abundance" of mineral deposits could be explained as produced by the fluids released via dehydration of the subducting oceanic crust in a shallow setting added

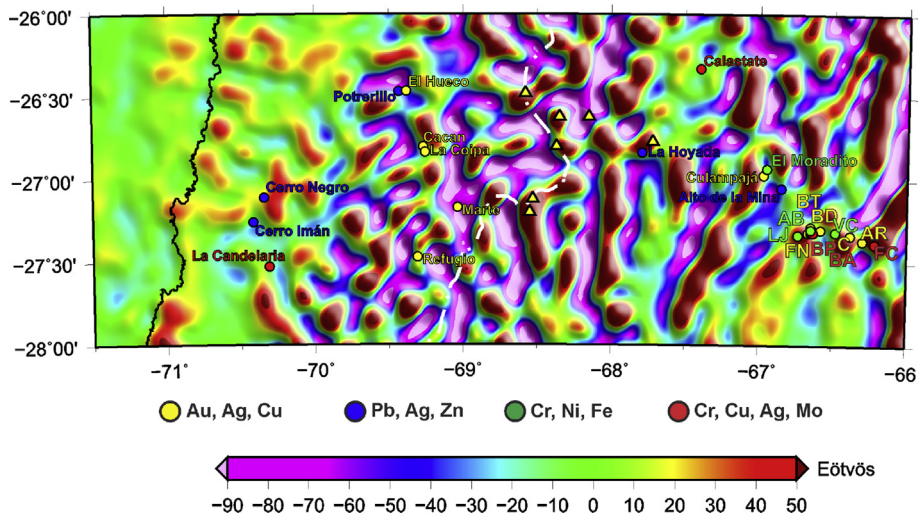

Fig. 4. Tzz from EIGEN-6C4 corrected by topographic effect in the region of the Copiapó ridge and Ojos del Salado-San Buena Ventura volcanic lineament. The track of the Copiapó ridge (black dashed line) is related to the most significant mining deposits in this region of Chile and Argentina. References: BT: Bajo la Tapada, BD: Bajo el Durazno, AR: Agua Rica, FN: Farallón Negro, C: Capillitas, BP: Bajo la Pampita, BA: Bajo la Alumbrera, FC: Filo Colorado, AB: Alto la Blenda, VC: Veta Carmen, LJ: La Josefa.

to a higher degree of mantle melting produced by a thicker oceanic crust resulted from seamounts compensation.

Conflicts of interests

The authors declare that there is no conflict of interest.

Acknowledgments

Authors greatly acknowledge the use of the GMT-mapping software of Wessel & Smith [52]. The authors thank CONICET and the National University of San Juan for their financial support.

Appendix A. Supplementary data

Supplementary data to this article can be found online at https://doi.org/10.1016/j.geog.2019.04.007.

References

[1] G.A. Yañez, C.R. Ranero, R. von Huene, J. Diaz, Magnetic anomaly interpretation across the southern Central Andes (32°–34° S): the role of the Juan Fernandez Ridge in the late Tertiary evolution of the margin, J. Geophys. Res. Solid Earth 106 (B4) (2001) 6325–6345.

[2] S.M. Kay, B. Coira, Shallowing and steepening subduction zones, continental lithospheric loss, magmatism, and crustal flow under the Central Andean Altiplano-Puna Plateau, in: S. Kay, V.A. Ramos, W. Dickinson (Eds.), Backbone of the Americas: Shallow Subduction Plateau Uplift and Ridge and Terrane Collision, vol. 204, Geological Society of America, Memoir, 2009, pp. 229–259.

[3] O. Álvarez, M. Gimenez, A. Folguera, S. Spagnotto, E. Bustos, W. Baez, C. Braitenberg, New evidence about the subduction of the Copiapó ridge beneath South America, and its connection with the Chilean-Pampean flat slab, tracked by satellite GOCE and EGM2008 models, J. Geodyn. 91 (2015) 65–88, https://doi.org/10.1016/j.jog.2015.08.002.

[4] S. Kay, B. Coira, C. Mpodozis, Field trip guide: neogene evolution of the Central Andean Puna plateau and southern central volcanic zone, in: S. Kay, V.A. Ramos (Eds.), Field Trip Guides to the Backbone of the Americas: Shallow Subduction Plateau Uplift and Ridge and Terrane Collision, vol. 13, Geological Society of America, Field Trip Guide, 2008, pp. 117–181.

[5] C. Mpodozis, S.M. Kay, M. Gardeweg, B. Coira, Geología de la región de Ojos del Salado (Andes centrales, 27°S): implicancias de la migración hacia el este del frente volcánico Cenozoico Superior, in: Proceedings, XIII Congreso Geológico Argentino, vol. 3, Asociación Geológica Argentina, Buenos Aires, Argentina, 1996, pp. 539–554.

[6] R. Seggiaro, F. Hongn, A. Folguera, J. Clavero, Hoja Geológica 2769 - II. Paso de San Francisco. Boletín 294, Programa Nacional de Cartas Geológicas 1:250.000, SEGEMAR - Servicio Nacional de Geología y Minería Argentino, Instituto de Geología y Recursos Minerales, Buenos Aires, 2000, 52 p.

[7] M. Zentilli, Geological evolution and metallogenic relationships in the Andes of Northern Chile between 26° and 29° South, Queen's University, Kingston, Ont, 1974, p. 446 (Ph.D. thesis).

[8] H. Gerth, Der geologische Bau der sudamerikanischen Kordillere, Borntraeger, Berlin, 1955.

[9] W.D. Carter, Evaluation of ERTS-1 Data: Applications to Geologic Mapping of S. America, with Emphasis on the Andes Mountain Region, Open File Report, U.S. Geol. Surv., Reston, Va, 1974.

[10] E. Bonatti, C.G.A. Harrison, D.E. Fisher, J. Honnorez, J.G. Schilling, J.J. Stipp, M. Zentilli, Easter volcanic chain (southeast Pacific): a mantle hot line, J. Geophys. Res. 82 (17) (1977) 2457–2478.

[11] C. Mpodozis, M.S. Kay, Late Paleozoic to Triassic evolution of the Gondwana margin: evidence from Chilean frontal Cordilleran Batholiths (28°–31°S), Geol. Soc. Am. Bull. 104 (1992) 999–1014.

[12] R. Marret, R. Allmendinger, R. Alonso, R. Drake, Late Cenozoic tectonic evolution of the Puna plateau and adjacent foreland, northwestern Argentine Andes, J. South Am. Earth Sci. 7 (1994) 179–208.

[13] O. González-Ferrán, P.E. Baker, D.C. Rex, Tectonic-volcanic discontinuity at latitude 27° South, Andean Range, associated with Nazca plate subduction, Tectonophysics 112 (1985) 423–441.

[14] P.E. Baker, O. González Ferrán, D.C. Rex, Geology and geochemistry of the Ojos del Salado volcanic region, Chile, J. Geol. Soc. London 144 (1987) 85–96.

[15] D. Comte, H. Haessler, D. Louis, M. Pardo, T. Monfret, A. Lavenu, B. Pontoise, Y. Hello, Seimicity and stress distribution in the Copiapó, northern Chile subduction zone using combined on- and off-shore seismic observations, Phys. Earth Planet. Interiors 123 (2002) 197–217.

[16] O. Álvarez, M. Giménez, A. Folguera, S. Spagnotto, C. Braitenberg, El ridge Copiapó y su relación con la cadena volcánica ojos del salado-buena ventura, y con la zona de subducción plana pampeana. Simposio S20: Subducción horizontal en el segmento andino 27°-33°S: Un enfoque multidisciplinario, XIX Congreso Geológico Argentino, Córdoba 2014, Exposición Oral, 2014, ISBN 978-987-22403-5-6.

[17] P. Mulcahy, C. Chen, S.M. Kay, L.D. Brown, B.L. Isacks, E. Sandvol, B. Heit, X. Yuan, B.L. Coira, Central Andean mantle and crustal seismicity beneath the Southern Puna plateau and the northern margin of the Chilean-Pampean flat slab, Tectonics 33 (2014) 1636–1658, https://doi.org/10.1002/2013TC003393.

[18] G. Rosenbaum, D. Giles, M. Saxon, P. Betts, R. Weinberg, C. Duboz, Subduction of the Nazca ridge and the Inca plateau: insights into the formation of ore deposits in Peru, Earth Planet. Sci. Lett. 239 (2003) 18–32.

[19] Christoph Förste, Sean L. Bruinsma, Oleg Abrikosov, Jean-Michel Lemoine, Jean Charles Marty, Frank Flechtner, et al., EIGEN-6C4 the Latest Combined Global Gravity Field Model Including GOCE Data up to Degree and Order 2190 of GFZ Potsdam and GRGS Toulouse, GFZ Data Services, 2014. https://doi.org/10.5880/ICGEM.2015.1.

[20] X. Li, Vertical resolution: gravity versus vertical gravity gradient, Lead. Edge 20 (8) (2001) 901–904.

[21] B. Hofmann-Wellenhof, H. Moritz, Physical Geodesy, second ed., Springer, Berlin, 2006, p. 286pp.

[22] F. Barthelmes, Definition of Functionals of the Geopotential and Their Calculation from Spherical Harmonic Models: Theory and Formulas Used by the Calculation Service of the International Centre for Global Earth Models (ICGEM), Deutsches GeoForschungsZentrum GFZ, Potsdam, 2013, p. 32, revised Edition (Scientific Technical Report ; 09/02), http://icgem.gfzpotsdam.de/ICGEM/, https://doi.org/10.2312/GFZ.b103-0902-26.

[23] J. Janak, M. Sprlak, New Software for Gravity Field Modelling Using Spherical Armonic: Geodetic and Cartographic Horizon, vol. 52, 2006, pp. 1–8 (in Slovak).
[24] N.K. Pavlis, S.A. Holmes, S.C. Kenyon, J.K. Factor, An Earth gravitational model to degree 2160: EGM2008, in: Proceedings, General Assembly of the European Geosciences Union: Vienna, Austria, 2008, 2008.
[25] C. Amante, B.W. Eakins, ETOPO1 1 Arc-Minute Global Relief Model: Procedures, Data Sources and Analysis, National Geophysical Data Center, NESDIS, NOAA, U.S. Department of Commerce, Boulder, CO, 2008.
[26] E.G. Anderson, The Effect of Topography on Solutions of Stokes' Problem, Unisurv S-14, Rep, School of Surveying, University of New South Wales, Kensington, 1976.
[27] B. Heck, K. Seitz, A comparison of the tesseroid, prism and point mass approaches for mass reductions in gravity field modeling, J. Geod. 81 (2) (2007) 121–136, https://doi.org/10.1007/s00190-006-0094-0.
[28] F. Wild-Pfeiffer, A comparison of different mass element for use in gravity gradiometry, J. Geod. 82 (2008) 637–653, https://doi.org/10.1007/s00190-008-0219-8.
[29] T. Grombein, B. Heck, K. Seitz, Untersuchungen zur effizienten Berechnung topographischer Effekte auf den Gradiententensor am Fallbeispiel der Satellitengradiometriemission GOCE, 7547, Karlsruhe Institute of Technology, KIT Scientific Reports, 2010, ISBN 978-3-86644-510-9, pp. 1–94.
[30] T. Grombein, B. Heck, K. Seitz, Optimized formulas for the gravitational field of a tesseroid, J. Geod. 87 (2013), 645-600.
[31] L. Uieda, N. Ussami, C.F. Braitenberg, Computation of the gravity gradient tensor due to topographic masses using tesseroids, in: Proceedings, Meet. Am. Suppl., Eos Trans., AGU, vol. 91, 2010 no. 26, Abstract G22A-04.
[32] L. Uieda, V.C. Barbosa, C.F. Braitenberg, Tesseroids: forward modeling gravitational fields in spherical coordinates, Geophysics 81 (5) (2016) F41–F48, https://doi.org/10.1190/GEO2015-0204.1.
[33] O. Álvarez, M. Gimenez, C. Braitenberg, Nueva metodologıa para el cálculo del efecto topográfico para la corrección de datos satelitales, Rev. Asoc. Geol. Argent. 70 (2013) 499–506.
[34] J. Bouman, J. Ebbing, M. Fuchs, Reference frame transformation of satellite gravity gradients and topographic mass reduction, J. Geophys. Res. Solid Earth 118 (2) (2013) 759–774, https://doi.org/10.1029/2012JB009747.
[35] P. Wessel, Global distribution of seamounts inferred from gridded Geosat/ERS-1 altimetry, J. Geophys. Res. 106 (B9) (2001) 19431–19441.
[36] R.D. Müller, M. Sdrolias, C. Gaina, W.R. Roest, Age, spreading rates, and spreading asymmetry of the world's ocean crust, Geochem. Geophys. Geosyst 9 (2008) 18–36.
[37] L. Siebert, T. Simkin, Volcanoes of the World: an Illustrated Catalog of Holocene Volcanoes and their Eruptions, Smithsonian Institution, Global Volcanism Program Digital Information Series, GVP-3, 2002. http://www.volcano.si.edu/world/.
[38] P. Wessel, L.W. Kroenke, A geometric technique for relocating hotspots and refining absolute plate motions, Nature 387 (1997) 365–369.
[39] P. Wessel, L.W. Kroenke, The geometric relationship between hot spots and seamounts: implications for Pacific hot spots, Earth Planet. Sci. Lett. 158 (1998) 1–18.
[40] P. Wessel, New Hotspotting tools released, Proceedings, EOS Trans. AGU 80 (29) (1999) 319.
[41] P. Wessel, Hotspotting: principles and properties of a plate tectonic Hough transform, Geochem. Geophys. Geosyst. 9 (2008) Q08004, https://doi.org/10.1029/2008GC002058.
[42] C. DeMets, R.G. Gordon, D.F. Argus, Geologically current plate motions, Geophys. J. Int. 181 (2010) 1–80, https://doi.org/10.1111/j.1365-246X.2009.04491.x.
[43] A.B. Watts, A.P. Kopper, D.P. Robinson, Seamount subduction and earthquakes, Oceanography 23 (1) (2010) 166–173.
[44] A. Nishizawa, K. Kaneda, N. Watanabe, M. Oikawa, Seismic structure of the subducting seamounts on the trench axis: Erimo Seamount and Daiichi-Kashima Seamount, northern and southern ends of the Japan trench, Earth Planets Space 61 (2009) e5–e8.
[45] E. Contreras-Reyes, I. Grevemeyer, A.B. Watts, L. Planert, E.R. Flueh, C. Peirce, Crustal intrusion beneath the Louisville hotspot track, Earth Planet. Sci. Lett. 289 (2010) 323–333.
[46] E. Kendrick, M. Bevis, R. Smalley, B. Brooks, R. Barriga, E. Lauri, The Nazca – south America Euler vector and its rate of change, J. South Am. Earth Sci. 16 (2003) 125–131.
[47] S. Kay, C. Mpodozis, Central Andean ore deposits linked to evolving shallow subduction systems and thickening crust, GSA Today (Geol. Soc. Am.) 4–9 (2001). GGSA GSA Today, March 2001SA Today, March 2001.
[48] I. Santibáñez, J. Cembrano, T. García-Pérez, C. Costa, G. Yáñez, C. Marquardt, G. Arancibia, G. González, Crustal faults in the Chilean Andes: geological constraints and seismic potential, Andean Geol. 46 (1) (2019) 32–65, https://doi.org/10.5027/andgeoV46n1-3067.
[49] D. Angermann, J. Klotz, C. Reigber, Space-geodetic estimation of the Nazca-south America Euler vector, Earth Planet. Sci. Lett. 171 (1999) 329–334.
[50] R. Roy, R.D. Cassard, P.R. Cobbold, E.A. Rossello, M. Billa, L. Bailly, A.L.W. Lips, Predictive Mapping for Copper–Gold Magmatic-Hydrothermal Systems in NW Argentina: Use of a Regional-Scale GIS, Application of an Expert-Guided Data-Driven Approach, and Comparison with Results from a Continental-Scale GIS, 2006.
[51] S.M. Kay, C. Mpodozis, V.A. Ramos, F. Munizaga, Magma source variations for mid-late Tertiary magmatic rocks associated with a shallowing subduction zone and thickening crust in the Central Andes (28-33°S), in: R.S. Harmon, C.W. Rapela (Eds.), Andean Magmatism and its Tectonic Setting: Special Paper of the Geological Society of America, vol. 26, 1991, pp. 113–137.
[52] P. Wessel, W.H.F. Smith, New, improved version of the generic mapping tools released, in: Proceedings, EOS Trans, AGU, vol. 79, 1998, p. 579, no. 47.

Gimenez, Mario Ernesto, San Juan, República Argentina, mgimenez@unsj-cuim.edu.ar, gimmario@gmail.com. Work: Professor in National University of San Juan, research in potential methods, 2004–2019. Principal research in National Council of Scientific and Technical Research (CONICET).